Antarctic Science 34(4), 313–324 (2022) doi:10.1017/S0954102022000177

The morphology of pockmarks on the north-east Antarctic Peninsula continental shelf

CHRISTINE L. BATCHELOR [1], BÉTINA A.V. FRINAULT [2], FRAZER D.W. CHRISTIE [3], ALEKSANDR MONTELLI [3] and JULIAN A. DOWDESWELL [3]

[1] *School of Geography, Politics and Sociology, Newcastle University, Newcastle upon Tyne NE1 7RU, UK*
[2] *School of Geography and the Environment, University of Oxford, Oxford OX1 3QY, UK*
[3] *Scott Polar Research Institute, University of Cambridge, Cambridge CB2 1ER, UK*
christine.batchelor@newcastle.ac.uk

Abstract: Pockmarks are sea-floor depressions that form when gas or liquid escapes from underlying sediments. Although they are a common feature of both glaciated and lower-latitude continental shelves, pockmarks have not been reported previously from the north-east Antarctic Peninsula margin. Here we use high-resolution geophysical data acquired using autonomous underwater vehicles to map > 240 pockmarks in three locations along the north-east Antarctic Peninsula shelf. The pockmarks are 0.4–45 m wide and 0.1–2.5 m deep, encompassing both smaller unit-pockmarks and larger normal-pockmarks. The high resolution of our data enables the identification of subdued features associated with the pockmarks, including acoustic flares within the water column, ejecta rims, intra-pockmark blocks and possibly even biological structures. The overprinting of subglacial and ice-marginal landforms by the pockmarks constrains their timing of formation to the last ~11 ka. The high density of pockmarks within the surveyed areas, together with geophysical evidence for the active seepage of gas to the sea floor, suggests that the expulsion of subsurface fluids is a widespread process on the north-east Antarctic Peninsula shelf that could have important implications for benthic biodiversity and the global carbon cycle.

Received 30 November 2021, accepted 23 March 2022

Key words: autonomous underwater vehicles, bathymetry, benthic biodiversity, Larsen continental shelf, Larsen Ice Shelf, submarine geomorphology

Introduction

Pockmarks are circular to elliptical depressions that are formed due to liquid or gas escaping from underlying sediments to the sea floor (Hovland & Judd 1988, Judd & Hovland 2009). These features occur in most marine and lake settings and have been reported from many glaciated margins (Hovland 1981, Solheim & Elverhøi 1993, Bünz *et al.* 2012, Dowdeswell & Vásquez 2013, Mazzini *et al.* 2016, Brown *et al.* 2017). Pockmark dimensions range from small 'unit-pockmarks' that are < 5 m wide to larger 'normal-pockmarks' that can reach several kilometres in diameter (Hovland & Judd 1988, Hovland *et al.* 2010). Pockmarks have been observed as isolated features, in linear to curvilinear chains that are linked to zones of weakness in underlying sediments, or in fields of up to several hundred closely spaced depressions (Hovland 1981, Chand *et al.* 2016).

Where they are preserved on or close to the sea floor, pockmarks indicate areas that are hydraulically active or have undergone expulsion of gas or liquid in the recent geological past. In continental shelf settings, pockmarks are commonly produced by gas-hydrate dissociation, the migration of biogenic or thermogenic gases and/or the upwelling of porewater from porous marine sediments (Hovland 1981, Solheim & Elverhøi 1993, Bünz *et al.* 2012, Mazzini *et al.* 2016). The release of methane and other greenhouse gases from pockmarks can result in positive feedback on climate warming (Wadham *et al.* 2012, 2019). Pockmarks can also influence benthic biodiversity and species distribution by increasing the sea-floor surface area, delivering nutrients, and providing a hard surface for colonization (Dando *et al.* 1991, Webb *et al.* 2009).

Despite their implications for the global carbon cycle and benthic communities, very little is known about fluid-escape structures, including pockmarks, on the Antarctic margin (García *et al.* 2009, Lawver *et al.* 2012, Giustiniani *et al.* 2017). Although a chemotrophic ecosystem has been linked to the sea-floor expulsion of thermogenic methane in Larsen B Embayment (Fig. 1; Domack *et al.* 2005, Niemann *et al.* 2009), no

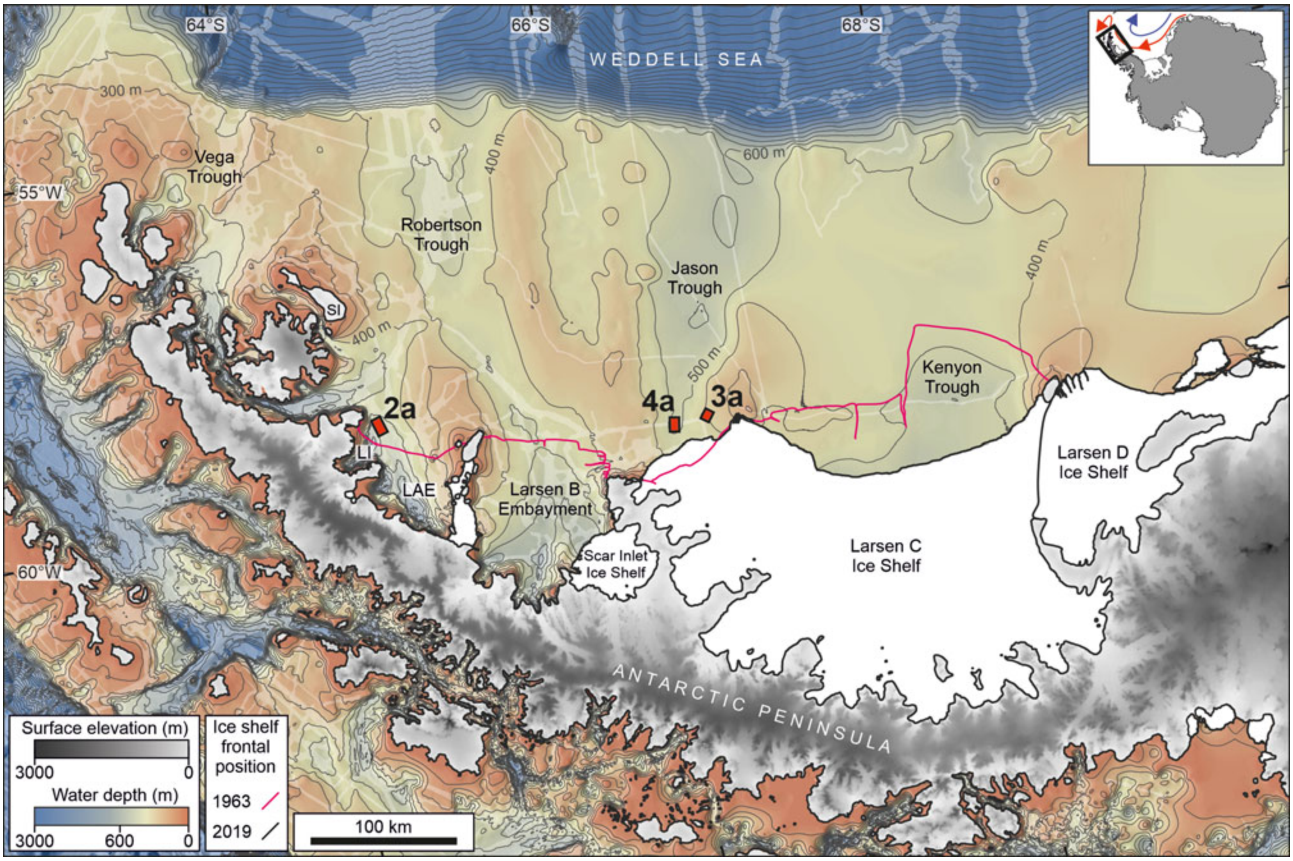

Fig. 1. Location of the three autonomous underwater vehicle surveys (red boxes) on the north-east Antarctic Peninsula continental shelf. Bathymetry is from the International Bathymetric Chart of the Southern Ocean (Arndt *et al.* 2013), with 100 m contours. Translucent shading shows existing bathymetric data coverage. Surface elevation is from the Reference Elevation Model of Antarctica (Howat *et al.* 2019). Modern ice shelves are shown in white and ice-covered land is shown with grey shading, darkening with increasing altitude. The Antarctic grounding line is from Depoorter *et al.* (2013). The ice-shelf frontal margins are from Cook & Vaughan (2010) and Christie *et al.* (2022). Inset shows the location of the study area (black box) in Antarctica. The blue arrow is the Weddell Gyre and the red arrow is the Weddell Slope Current. LAE = Larsen A Embayment; LI = Larsen Inlet; SI = Seymour Island.

pockmarks have been reported previously from the north-east Antarctic Peninsula continental shelf. This apparent absence of pockmarks is probably related, in part at least, to the low data coverage of this region of the Southern Ocean, which often remains covered by sea ice even during the austral summer (Dowdeswell *et al.* 2020b). Ship-based operations on the north-east Antarctic Peninsula shelf have also generally acquired bathymetric data that have a horizontal resolution of several tens of metres (Evans *et al.* 2005, Lavoie *et al.* 2015), from which it may not be possible to identify subdued features such as pockmarks on the sea floor.

Here we use high-resolution geophysical data acquired from autonomous underwater vehicles (AUVs) to map > 240 pockmarks in three locations on the north-east Antarctic Peninsula continental shelf (Fig. 1). The distribution, morphology and probable age of these features are discussed in terms of the implications for subsurface fluid flow and benthic biodiversity in this glaciated shelf environment.

Background

Geological setting and glacial history

The inner continental shelf of the north-east Antarctic Peninsula, which reaches water depths of > 1000 m (Fig. 1), is characterized by narrow sedimentary basins and outcrops of exposed to near-surface bedrock (Evans *et al.* 2005, Lavoie *et al.* 2015). There is a seaward transition to a mid- to outer-shelf sedimentary substrate that comprises prograding units of mainly glacigenic sediments (Smith & Anderson 2010). The continental shelf is incised by four major cross-shelf troughs that are generally between 400 and 600 m deep and are separated by shallower banks (Fig. 1). The troughs were eroded by ice streams (fast-flowing corridors of ice) of the Antarctic Peninsula Ice Sheet during successive full-glacial periods (Ó Cofaigh *et al.* 2014).

The distribution of glacial landforms preserved on the sea floor has revealed that the Antarctic Peninsula Ice Sheet extended to the shelf break during the Last

https://doi.org/10.1017/S0954102022000177 Published online by Cambridge University Press

Glacial Maximum (~20 ka; Evans *et al.* 2005, Ó Cofaigh *et al.* 2014, Lavoie *et al.* 2015). Relative palaeomagnetic intensity and radiocarbon dating of sediment cores suggest that the transition from grounded to floating ice was established in Larsen A and B embayments (Fig. 1) by ~11 ka (Brachfeld *et al.* 2003, Evans *et al.* 2005, Ó Cofaigh *et al.* 2014). The eastern Antarctic Peninsula Ice Sheet had retreated westwards across the shelf to approximately its present-day configuration by ~10 ka (Ó Cofaigh *et al.* 2014).

An overall reduction in the area of the floating ice shelves that fringe the north-east Antarctic Peninsula has been observed since the onset of the satellite observational era in the early 1960s (Fig. 1; Cook & Vaughan 2010, Christie *et al.* 2022). Major ice-shelf collapses, which have been linked to atmospheric and ocean forcing, occurred in the Larsen Inlet, Larsen A Embayment and Larsen B Embayment regions in 1989, 1995 and 2002, respectively (Cook & Vaughan 2010, Christie *et al.* 2022).

Sea-floor sedimentological and oceanographic conditions

The shallow stratigraphy of the continental shelf comprises a thin (1–8 m) drape of glacimarine sediment that overlies a unit of subglacial traction till (Evans *et al.* 2005, Batchelor *et al.* 2020). Iceberg ploughmarks, formed by the grounding of iceberg keels in soft sea-floor sediments, have incised the sea floor in water depths down to ~600 m and are particularly common on the shallow banks that separate the troughs (Dowdeswell *et al.* 2020b). The sea floor is covered intermittently by clasts of ice-rafted debris that are up to 1 m wide (Domack *et al.* 2005, Batchelor *et al.* 2020).

The present-day oceanography of the north-east Antarctic Peninsula is controlled by the cyclonic-flowing Weddell Gyre, which modifies and transports relatively warm, high-salinity Circumpolar Deep Water to this region in the form of Warm Deep Water via the Weddell Slope Current (inset in Fig. 1; Vernet *et al.* 2019). Together with overlying surface winds, the clockwise circulation of the Weddell Gyre also influences the northwards drift of icebergs and sea ice along this margin. At depth, cold and dense Weddell Sea Bottom Water is formed locally by sea-ice formation and contact with eastern Antarctic Peninsula ice shelves, whilst a layer of Antarctic Surface Water or mixed Winter Water occupies the upper ~200 m of the water column (Nicholls *et al.* 2009).

Data and methods

Geophysical data acquisition from AUVs

Two Kongsberg HUGIN 6000 AUVs were used to acquire geophysical data from three sites on the north-east Antarctic Peninsula continental shelf (Fig. 1). Data were collected beyond Larsen Inlet at ~550 m water depth (Fig. 2), at the southern margin of Jason Trough at ~350 m water depth (Fig. 3) and along the central axis of Jason Trough at ~550 m water depth (Fig. 4).

The AUV that acquired data from Larsen Inlet and the southern margin of Jason Trough was equipped with a Kongsberg EM2040 multi-beam echo-sounder that was operated at 400 kHz and an EdgeTech 2205 75 kHz side-scan sonar system. The AUV maintained fixed separation distances from the sea floor of 70 and 60 m in Larsen Inlet and southern Jason Trough, respectively. Approximately 9 km^2 of bathymetric data were acquired from Larsen Inlet (Fig. 2a), whilst 0.6 km^2 of bathymetric data and ~0.3 km^2 of side-scan sonar data were collected from the southern margin of Jason Trough (Fig. 3a). Processing of the multi-beam echo-sounder and navigation data was performed using *EIVA* and *Navlab* software and included adjustments for tidal variations relative to the WGS85 Ellipsoid and a low-pass filter to remove erroneous depth soundings. The bathymetric data have a horizontal resolution of ~0.5 m and are gridded with a cell size of 1 m.

The second AUV, which was deployed in central Jason Trough, was equipped with a high-resolution interferometric synthetic aperture sonar (HISAS) system that was operated at a frequency range of 60–120 kHz. The AUV maintained a fixed separation distance of 25 m from the sea floor and acquired ~4 km^2 of HISAS backscatter images that have a horizontal resolution of ~0.05 m. In addition, the interferometric capability of the HISAS system enabled these images to be processed to produce bathymetry with a gridded cell size of 1 m (Fig. 4a). The data were examined for evidence of acoustic reflections within the water column prior to data processing using *Delph* software.

Both AUVs were equipped with an EdgeTech Chirp sub-bottom profiler with a bandwidth of 1–11 kHz and a pulse length of 20 ms. Approximately 64 line-km, 2 line-km and 13 line-km of sub-bottom profiler data were acquired from Larsen Inlet, southern Jason Trough and central Jason Trough, respectively (Figs 2a, 3a & 4a). The sub-bottom profiler data have a horizontal resolution of ~0.5 m and a vertical resolution of ~0.1 m. Additional details about the AUV equipment deployed in this study are presented in Batchelor *et al.* (2020) and Dowdeswell *et al.* (2020a).

Pockmark mapping and analysis

Geomorphological mapping of sea-floor depressions was performed manually using standard geographical information software. To ensure that we did not map 'ping dropouts' on the bathymetric data, we did not include sea-floor depressions that have a diameter of

< 4 m (four grid cells). Smaller pockmarks may therefore exist beneath the resolution of the AUV-acquired data.

Pockmark width was measured from the break in slope that defines the central depression rather than from the crest of any rims, which can extend up to several metres beyond the pockmark edge (e.g. Fig. 2c). Width was measured across the widest part of each depression. Pockmark depth, which was only measured where bathymetric data were available, was defined as the vertical distance from the break in slope to the bottom of the depression. Width and depth were recorded to the nearest metre and tenth of a metre, respectively. To examine the relationship between pockmark size and water depth (Fig. 5b; e.g. Chand *et al.* 2016), sea-floor depth values were acquired from the centre of each depression.

Results

A total of 245 circular to elliptical sea-floor depressions are mapped within the three AUV survey sites (Figs 2–4). These features are between 0.4 and 45 m wide and between 0.1 and 2.5 m deep (Fig. 5). The majority are < 15 m wide and < 1 m deep.

The depressions are interpreted as pockmarks formed by the expulsion of fluid from underlying sediments to the sea floor (Hovland & Judd 1988, Judd & Hovland 2009). They are smaller and more circular than iceberg ploughmarks and plough pits (Fig. 3; e.g. Chand *et al.* 2016, Brown *et al.* 2017), and their negative relief precludes their interpretation as boulders of ice-rafted debris (Fig. 4b & c).

Larsen Inlet

Almost 200 circular pockmarks are mapped at ~550 m water depth in the outermost part of Larsen Inlet (Fig. 2a). These are superimposed upon an assemblage of glacial landforms that includes subglacially formed lineations and ice-marginal grounding-zone wedges (Fig. 2a–f; Evans *et al.* 2005, Batchelor *et al.* 2020, Dowdeswell *et al.* 2020a). The pockmarks occur mainly as isolated features, with an average density of 23 pockmarks per km^2. A cluster of closely spaced pockmarks, with a density of up to 76 pockmarks per km^2, is present in the central part of the surveyed area (Fig. 2a & f).

Some of the pockmarks have a fresh appearance on the bathymetric data (Fig. 2b–d). They are surrounded by small rims that are a few tens of centimetres high, a few metres wide and up to several tens of metres long (Fig. 2b–d). The rims typically fringe the pockmarks but can be located up to 10 m beyond the edge of the depression (Fig. 2c). They are interpreted as sediment that was ejected from the subsurface during fluid expulsion. Pockmarks with rims are rarely observed in the geological record because the ejected sediment is typically redistributed by ocean currents soon after it is deposited (Hovland *et al.* 2002). Some of the surveyed pockmarks are 'eyed pockmarks' that have a small ridge within their central depression (Fig. 2c; Hovland *et al.* 2002). These ridges could be accumulations of ejected sediment or carbonate blocks formed by microbiologically induced carbonate precipitation (Mazzini *et al.* 2016). Collectively, the preservation of these fresh-looking (i.e. unburied) subdued features on the sea floor suggests that at least some of the pockmarks in Larsen Inlet are recently formed or are experiencing ongoing fluid seepage to maintain their structure.

Other pockmarks in outer Larsen Inlet have poorly defined margins on the bathymetric data (Fig. 2e), which suggests that they are draped by a layer of glacimarine sediment. An average post-glacial sedimentation rate of ~0.1 m per 1000 years is suggested from sub-bottom profiles and sediment cores in Larsen Inlet that record a 1 m-thick unit of glacimarine sediment overlying subglacial traction till (Fig. 2 g & h; Evans *et al.* 2005, Batchelor *et al.* 2020).

Southern margin of Jason Trough

A total of 45 pockmarks are mapped at the southern lateral margin of Jason Trough (Fig. 3a). These features, which are located at ~350 m water depth, have similar dimensions to the pockmarks in the deeper Larsen Inlet (Fig. 5b). All of the pockmarks in southern Jason Trough occur outside the margins of linear to curvilinear depressions that are interpreted to have been produced by the grounding of iceberg keels in sea-floor sediments (Fig. 3a & c; Batchelor *et al.* 2020). The depth of these iceberg ploughmarks (~350 m) suggests that they were produced during the last deglaciation (Dowdeswell *et al.* 2020b).

The pockmarks at the southern margin of Jason Trough have relatively indistinct margins (Fig. 3b & c), which suggests that they may not be active at present. This is unlikely to be a consequence of burial by glacimarine sediments because sub-bottom profiles show minimal post-glacial sedimentation in this area (Fig. 3e). Alternatively, it is possible that the lack of well-defined pockmark rims is linked to the removal of material by strong ocean currents; the high-amplitude sea-floor reflection on acoustic images (Fig. 3e) and the elliptical shape of some of the pockmarks (Fig. 3c) may indicate high bottom-current velocities across this relatively shallow bank (Hovland *et al.* 2002).

Central Jason Trough

Four pockmarks are mapped on the HISAS-derived bathymetry at ~500 m water depth in central Jason Trough (Fig. 4a). The pockmarks are superimposed

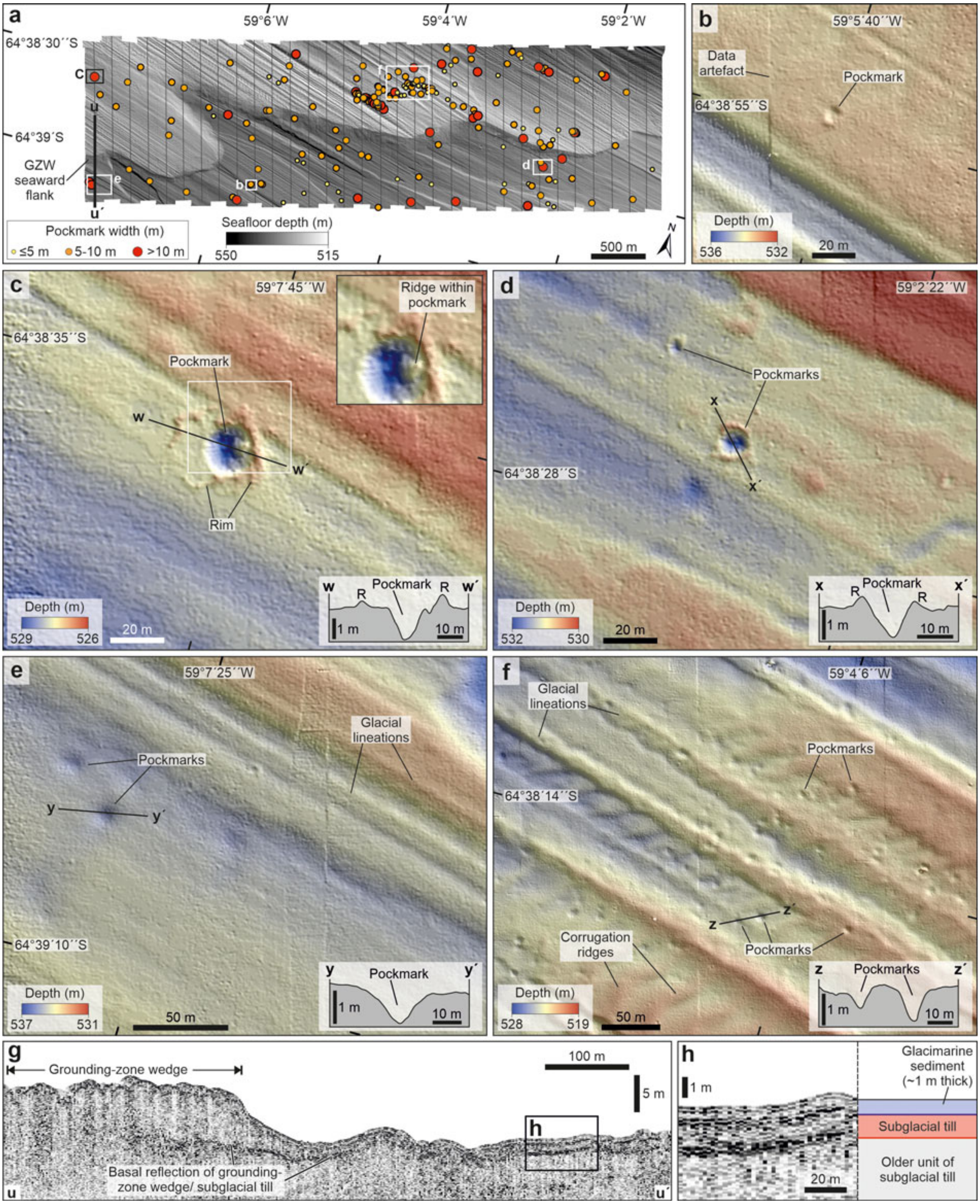

Fig. 2. Marine geophysical data acquired from outer Larsen Inlet (location in Fig. 1). **a.** Greyscale bathymetric data with grid cell size 1 m. Coloured circles show the locations of the 196 pockmarks mapped in the surveyed area. Vertical grey lines are autonomous underwater vehicle track lines. **b.–d.** Details of pockmarks surrounded by small rims that are a few tens of centimetres high (marked 'R' on inset cross profiles). **e.** Detail of pockmarks that may be shallowly buried. **f.** Detail of a cluster of small (< 5 m wide) pockmarks. **g.** Sub-bottom profile showing the shallow acoustic stratigraphy of Larsen Inlet (profile location in **a.**). **h.** Detail of the shallow acoustic stratigraphy alongside an interpretation of the various seismo-stratigraphic units. GZW = grounding-zone wedge.

https://doi.org/10.1017/S0954102022000177 Published online by Cambridge University Press

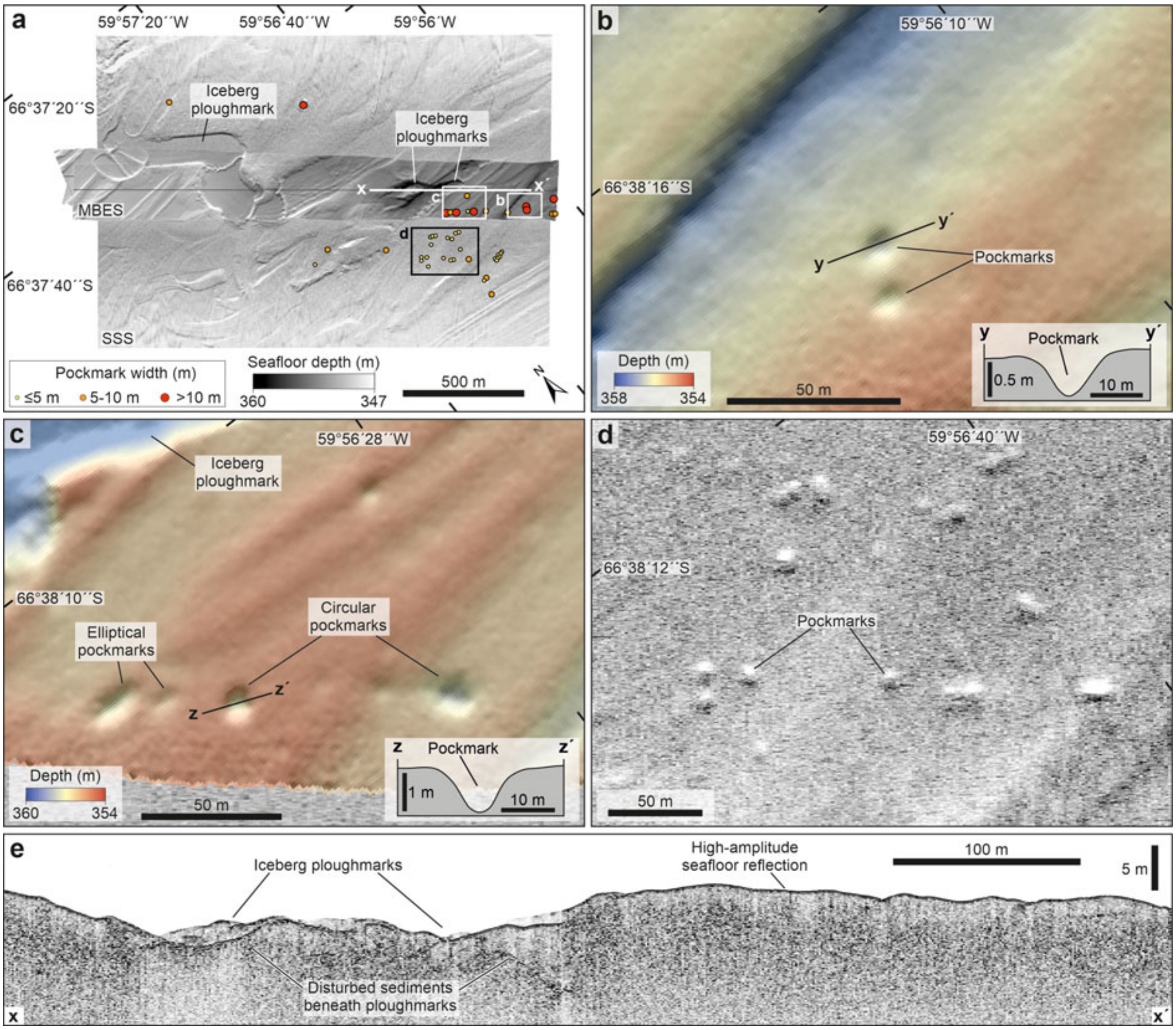

Fig. 3. Marine geophysical data acquired from the southern lateral margin of Jason Trough (location in Fig. 1). **a.** Greyscale multi-beam echo-sounder (MBES) and side-scan sonar (SSS) data. Grid cell size 1 m. Coloured circles show the locations of the 45 pockmarks mapped in the surveyed area. Thin grey lines are autonomous underwater vehicle track lines. **b.–d.** Details of pockmarks preserved on or close to the sea floor. **e.** Detail of the shallow acoustic stratigraphy (profile location in **a.**).

upon subglacially formed lineations that record the flow of a palaeo-ice stream in an easterly direction through Jason Trough from the Antarctic Peninsula (Batchelor *et al.* 2020).

HISAS images reveal the sea-floor expression of the pockmarks at high resolution (horizontal resolution of ~0.05 m; Fig. 4b & c). The two largest pockmarks, which are 45 and 22 m wide, have asymmetric shapes with higher and shallower-gradient northern sides and lower and steeper-gradient southern flanks (inset profile in Fig. 4c). They have an irregular surface morphology that includes several ridges (Fig. 4c). These internal structures are a common feature of active gas or liquid release systems and were probably formed by the disturbance of sea-floor sediments during fluid expulsion and/or the deposition of ejected sediments (Judd & Hovland 2009, Bünz *et al.* 2012).

A hydrologically active system is also suggested by the bathymetric data, which show acoustic reflections or 'flares' within the water column above the 45 m-wide pockmark (Fig. 4e). Several near-vertical flares are observed emanating from this large pockmark. They extend upwards from the sea floor several metres into the water column (Fig. 4e). Similar features have been identified emerging from pockmarks on the North Sea and western Svalbard margins, where they have been interpreted as gas plumes formed by the active seepage of gas to the sea floor (Bünz *et al.* 2012). Acoustic reflections in the water column can also indicate groundwater seepage where the groundwater has a

https://doi.org/10.1017/S0954102022000177 Published online by Cambridge University Press

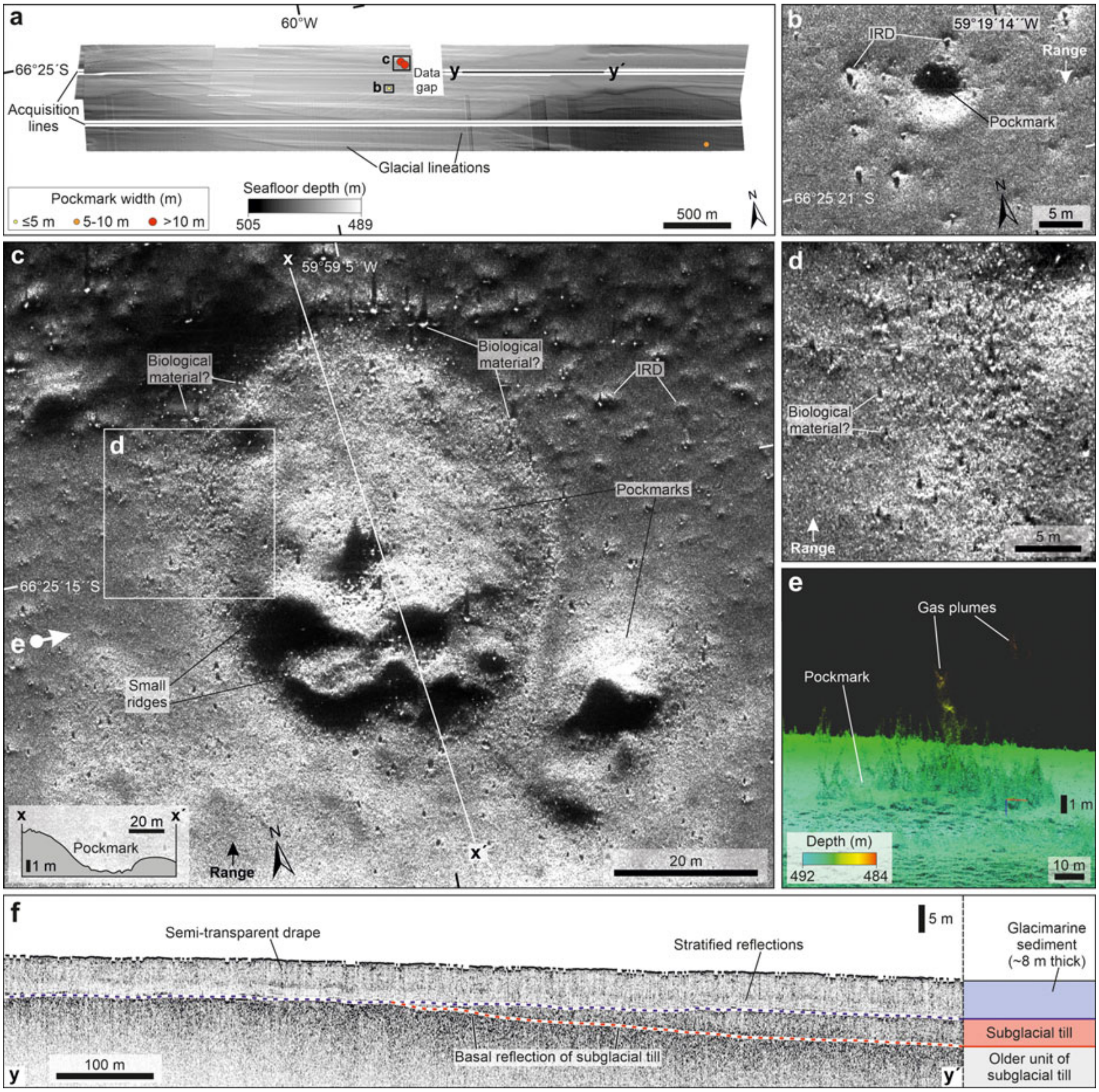

Fig. 4. Marine geophysical data acquired from central Jason Trough (location in Fig. 1). **a.** Greyscale high-resolution interferometric synthetic aperture sonar (HISAS)-derived bathymetric data with grid cell size 1 m. Coloured circles show the locations of the four pockmarks mapped in the surveyed area. Thin grey lines are autonomous underwater vehicle track lines. **b.** HISAS amplitude image of a 5 m-wide pockmark and boulders of ice-rafted debris (IRD) on the sea floor. The side-scan sonar look-direction was towards the south. **c.** HISAS amplitude image of two pockmarks in Jason Trough. The larger pockmark is 45 m wide and 2.5 m deep. The side-scan sonar look-direction was towards the north. **d.** Detail showing small positive-relief features at the edge of the pockmark, which may be biological material such as sponges or corals. **e.** Oblique view of pre-processed HISAS-derived bathymetric data (view direction shown in **c.**), showing reflection of the acoustic signal from gas plumes immediately above the large pockmark. **f.** Sub-bottom profile showing the shallow acoustic stratigraphy of Jason Trough (profile location in **a.**) alongside an interpretation of the various seismo-stratigraphic units.

different composition from the surrounding seawater (Hoffmann *et al.* 2020).

Whilst boulders of ice-rafted debris up to 1 m wide are scattered across the sea floor (Fig. 4b & c), smaller positive-relief structures appear to be clustered around the margins of the pockmarks (Fig. 4c & d). These structures are distinct from the ejecta rims that fringe some of the pockmarks in Larsen Inlet (Fig. 2b–d) because they are smaller (< 1 m wide) and comprise numerous individual features. In contrast, ejecta rims are typically a few metres wide and up to several tens of metres long, and they have a circular to elliptical

https://doi.org/10.1017/S0954102022000177 Published online by Cambridge University Press

plan-form shape (e.g. Fig. 2c). It is possible that the small features clustered around the margins of the pockmarks in central Jason Trough (Fig. 4b & c) are biological structures, such as deep-water sponges or cold-water corals. Such biological structures may benefit from the flow of oxygen-rich Weddell Sea Bottom Water over the elevated pockmark rims and/or the fertilization of the water by gas seepage to the sea floor (Webb *et al.* 2009). It is also possible that some of the small structures surrounding the pockmarks are accumulations of ejected sediment or authigenic carbonates (Mazzini *et al.* 2016).

Discussion

Pockmark distribution and morphology

Our AUV surveys represent small but morphologically diverse regions of the sea floor in trough and bank settings at water depths of between 350 and 550 m (Fig. 1). Pockmarks are present in all three surveyed areas, suggesting that they may be widespread along the north-east Antarctic Peninsula continental shelf (Fig. 1).

Approximately one-third (32%) of the pockmarks mapped in this study can be classified as unit-pockmarks that are ≤ 5 m in diameter (Fig. 5a; Hovland & Judd 1988, Hovland *et al.* 2010). These features are rarely identified from multi-beam bathymetric surveys because they are usually smaller than the resolution of hull-mounted sonar systems operating in water depths of a few hundred metres (e.g. Bünz *et al.* 2012, Dowdeswell & Vásquez 2013, Brown *et al.* 2017). Unit-pockmarks are interpreted to record the slow, diffuse and cyclic seepage of fluid to the sea floor (Hovland *et al.* 2010). The remaining two-thirds (68%) of the mapped pockmarks are normal-pockmarks. These larger structures are probably formed by more explosive and intermittent eruptions of excess fluid, which are separated by longer periods of diffuse and constant venting (Cathles *et al.* 2010, Hovland *et al.* 2010).

Unit-pockmarks are commonly identified within and around the margins of larger 'parental' features (Judd & Hovland 2009, Webb *et al.* 2009, Hovland *et al.* 2010), which has led to the suggestion that they form during the early stages of normal-pockmark development (Cathles *et al.* 2010). In this formation model, over-pressured fluid migrates initially through the weakest zones of the subsurface, producing unit-pockmarks, before the fluid chimney reaches close to the sea floor and erupts to form a normal-pockmark (Cathles *et al.* 2010). However, the distribution of pockmarks within our surveyed areas, in which both unit- and normal-pockmarks occur as isolated features and in clusters without a parental depression (Figs 2–4), suggests that unit-pockmark formation is not always

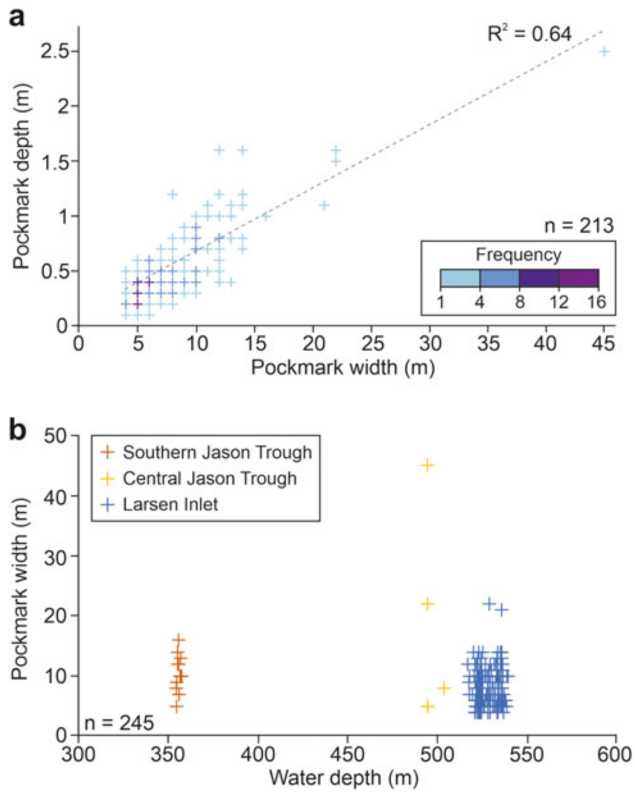

Fig. 5. Scatterplots showing the dimensions of the pockmarks mapped in this study. Note that we did not map pockmarks that are < 4 m wide. **a.** Scatterplot showing the relationship between pockmark width and pockmark depth. Colours correspond to frequency of observations. **b.** Scatterplot showing the relationship between water depth and pockmark width. Colours correspond to survey site.

followed by the development of larger structures (Hovland *et al.* 2010).

The scatter plot and least-squares regression fit shown in Fig. 5a demonstrate that pockmark width has a moderate positive correlation with pockmark depth (correlation coefficient of 0.64). These variables scale linearly because they are both related to the magnitude and explosivity of the fluid seepage event(s). Comprehensive analysis of the relationship between pockmark size and water depth (e.g. Chand *et al.* 2016) is precluded by the limited range of water depths within each small surveyed area (Fig. 5b). However, the lack of correlation observed between pockmark size and water depth *between* the surveyed areas (Fig. 5b) may reflect the similar shallow geology of these sites (Figs 2h, 3e & 4f).

Timing of pockmark formation

The overprinting of subglacial and ice-marginal landforms, including glacial lineations and grounding-zone wedges, by the pockmarks (Fig. 2c–f) constrains the timing of pockmark formation to within the last

11 ka, by which time grounded ice had probably retreated landwards of the surveyed areas following its presence along the shelf break during the Last Glacial Maximum (Brachfeld *et al.* 2003, Evans *et al.* 2005, Ó Cofaigh *et al.* 2014). Although small unit-pockmarks are easily masked by sediment infilling and have been suggested to have lifespans of only a few decades (Hovland *et al.* 2010), relatively low rates of post-glacial sedimentation on the north-east Antarctic Peninsula shelf (0.10–0.75 m per 1000 years; Evans *et al.* 2005, Batchelor *et al.* 2020) may have enabled them to persist for several thousands of years.

In the absence of subsurface acoustic features, it is not possible to constrain the timing of pockmark development relative to the formation of the iceberg ploughmarks at the southern lateral margin of Jason Trough (Fig. 3). If the pockmarks were produced prior to the iceberg ploughmarks, the disturbance and redistribution of sediment by iceberg keels could have removed sea-floor evidence for these depressions. Alternatively, if pockmark formation post-dated iceberg scouring, the pockmarks may have developed preferentially beyond the ploughmarks because sediment compaction by iceberg keels can impede upwards fluid flow (Chand *et al.* 2016).

The presence of both active and inactive pockmarks is interpreted within the surveyed areas. Some of the pockmarks have clearly defined margins on the bathymetric data and are associated with ejecta rims (Fig. 2c & d), which suggest that they are active at present or recently formed over perhaps the past few decades (Cathles *et al.* 2010, Hovland *et al.* 2010). In central Jason Trough, the presence of acoustic flares in the water column above a large pockmark (Fig. 4e) indicates the active seepage of gas to the sea floor (Judd & Hovland 2009, Bünz *et al.* 2012). Some of the other pockmarks have poorly defined margins (Figs 2e & 3b & c), which suggests that they are shallowly buried by glacimarine sediments and have probably become inactive.

Origins of the pockmarks

The sub-bottom profiles do not contain any acoustic features, such as pipes, chimneys or distortions, which could provide insights into the nature of the subsurface fluid flow systems identified in this study. In this section, we evaluate three mechanisms by which the pockmarks may have been formed.

Firstly, it is possible that some of the unit-pockmarks are formed by the compaction-driven upwelling of porewater from porous marine sediments (Böttner *et al.* 2019). However, the explosivity that is implied by the ejecta rims that surround some of the normal-pockmarks (Fig. 2c & d), together with the presence of acoustic flares above the large pockmark in central Jason Trough (Fig. 4e), suggest that the release of porewater is unlikely to be the sole mechanism for pockmark formation in this region.

Secondly, the pockmarks may be related to the production of methane by microbial activity in near-surface sediments. However, the sea floor is underlain by a thin (~1–8 m) layer of glacimarine sediment within the three survey sites (Figs 2h, 3e & 4f), and this material is not rich in organic matter (Brachfeld *et al.* 2003, Evans *et al.* 2005). Elevated concentrations of thermogenic methane, as opposed to microbial gas, have also been measured in near-sea-floor sediments in the neighbouring Larsen B Embayment (Fig. 1; Niemann *et al.* 2009).

Finally, pockmark formation may be related to deeper thermogenic processes. It is possible that extensive glacial erosion of the continental shelf has enabled connections to be made to migration pathways for methane and other gases generated from source rocks, which, in this location, include Mesozoic marine shales (Domack *et al.* 2005, Niemann *et al.* 2009). The pockmarks could also be produced by the dissociation of gas hydrates that were formed when migrating thermogenic gas entered a subsurface zone of gas-hydrate stability (Hovland *et al.* 2002, Winsborrow *et al.* 2016). Although the presence of gas hydrates has not been confirmed on the north-east Antarctic Peninsula margin, it has been inferred previously from the detection of methane within sea-floor sediments adjacent to Seymour Island (Fig. 1; del Valle *et al.* 2017). Gas-hydrate destabilization on glaciated margins has been linked to depressurization by the removal of grounded ice and the increase in ocean temperature that accompanied the last deglaciation (Solheim & Elverhøi 1993, Winsborrow *et al.* 2016, Böttner *et al.* 2019). The post-glacial age of the pockmarks on the north-east Antarctic Peninsula is consistent with an origin through gas-hydrate dissociation. The north-east Antarctic Peninsula shelf is also within the sea-floor depth range for hydrate stability on polar margins, which can extend down to ~2000 m (Majorowicz & Osadetz 2001).

Implications for gas-hydrate reserves and benthic biodiversity

Where a thermogenic origin is confirmed, the identification and monitoring of active pockmark fields on glaciated margins is important for predicting how global gas-hydrate reserves may evolve in a warming climate (Wadham *et al.* 2012, 2019). Given that gas-hydrate destabilization and methane release have been linked to past periods of ocean warming and ice-sheet retreat (Solheim & Elverhøi 1993, Winsborrow *et al.* 2016, Böttner *et al.* 2019), a future increase in ocean-water temperature and/or reduction in the extent of grounded ice around Antarctica could act as positive feedbacks on

https://doi.org/10.1017/S0954102022000177 Published online by Cambridge University Press

climate warming (Wadham *et al.* 2012, 2019). Conversely, higher rates of glacimarine sedimentation under warmer ocean and atmospheric conditions could reduce the flux of greenhouse gases from deep reservoirs to the sea floor by burying fluid-escape structures such as pockmarks, causing them to become inactive. The balance between these processes is particularly important on the Antarctic Peninsula, which has experienced one of the highest rates of atmospheric warming on the planet in recent decades (Cook & Vaughan 2010).

The high density of pockmarks identified from our AUV-derived geophysical data (Figs 2–4) suggests that the release of fluids from underlying sediments to the sea floor is a widespread process on the north-east Antarctic Peninsula margin, which could also have important implications for benthic biodiversity. Pockmarks, and the carbonate rocks that are often associated with them, can increase benthic biodiversity by enhancing the heterogeneity of the sea-floor habitat and providing hard rocks for colonization (Hovland & Judd 1988, Webb *et al.* 2009). Pockmarks can also provide unique habitats for the development of chemotrophic ecosystems that derive their metabolic energy from chemical reactions associated with vented fluids (chemosynthesis) rather than by photosynthesis (Dando *et al.* 1991, Webb *et al.* 2009, Bünz *et al.* 2012).

Although geochemical investigations are needed to confirm the active venting of fluid to the sea floor, some of the pockmarks mapped using our AUV-derived data may support similar chemosynthetic communities to those identified in the neighbouring Larsen B Embayment (Fig. 1; Domack *et al.* 2005, Niemann *et al.* 2009). An obvious target for future research is the large, potentially active pockmark in central Jason Trough (Fig. 4c & e), which appears to have a high density of biological structures (< 1 m wide) on its rims (Fig. 4d). Increased rates of ice-sheet decay, ice-shelf retreat and glacimarine sedimentation under warmer atmospheric and ocean temperatures may render these communities vulnerable to loss by pockmark infilling and burial (Domack *et al.* 2005, Niemann *et al.* 2009).

Conclusions

- Geophysical data acquired from AUVs are used to map > 240 pockmarks at high resolution in three areas on the north-east Antarctic Peninsula continental shelf (Figs 1–4).
- The high density (up to 76 pockmarks per km^2) of sea-floor depressions within the surveyed areas suggests that the venting of subsurface fluids to the sea floor is an important process on the north-east Antarctic Peninsula margin. A particularly significant subsurface plumbing system exists in Larsen Inlet, where almost 200 pockmarks are mapped within an area of ~9 km^2 (Fig. 2).
- The pockmarks are between 0.4 and 45 m wide and between 0.1 and 2.5 m deep (Fig. 5). They encompass small unit-pockmarks that are probably formed by the slow and cyclic seepage of fluid to the sea floor, and larger normal-pockmarks that record more explosive and intermittent fluid-escape events. The pockmarks occur as isolated features and in groups without a parental depression.
- The overprinting of subglacial and ice-marginal landforms by the pockmarks constrains the timing of pockmark formation to within the last ~11 ka, when grounded ice retreated landwards of the surveyed areas.
- At least some of the pockmarks are probably active or formed relatively recently, including in Larsen Inlet, where circular to elliptical ejecta rims are identified beyond well-defined pockmark edges (Fig. 2c & d). Acoustic flares, which are interpreted as gas plumes produced by the seepage of gas to the sea floor, are observed above a 45 m-wide pockmark in central Jason Trough (Fig. 4c & e). Smaller (< 1 m-wide) positive-relief features, which could be biological structures, are clustered on the rim of this active vent (Fig. 4d).
- Although the pockmarks mapped in this study could have been formed by compaction-related dewatering and/or microbial activity in near-surface sediments, the explosivity that is implied by their ejecta rims (Figs 2c & d & 4c), combined with elevated concentrations of thermogenic methane in near-sea-floor sediments in the neighbouring Larsen B Embayment (Fig. 1), suggest that their formation may be linked to the migration and escape of thermogenic gases.
- The prevalence of pockmarks on the north-east Antarctic Peninsula shelf may have implications for the marine biodiversity of this region, such as by providing refuges for benthic biodiversity and/or supporting unique chemotrophic ecosystems.

Acknowledgements

Autonomous underwater vehicle deployments were from the South African icebreaking research vessel S.A. *Agulhas II*, and we thank the captain, ice pilot, officers and crew for their support of our work. We thank John Howe and an anonymous reviewer for their helpful reviews of this manuscript.

Financial support

This research was funded by the Flotilla Foundation and Marine Archaeology Consultants Switzerland. The autonomous underwater vehicles and associated technical support were provided by Ocean Infinity and Deep Ocean Search. This paper was also produced with the financial assistance of the Prince Albert II of Monaco Foundation (to FDWC and JAD) and the Natural Environment Research Council (to BAVF).

Author contributions

CLB analysed the data, wrote the manuscript and produced the figures, with input from BAVF, FDWC, AM and JAD, each of whom took part in the field data acquisition programme.

Details of data deposit

Shapefiles showing the locations of the pockmarks mapped in this study are available on the Open Science Framework (https://osf.io/74YZT).

References

ARNDT, J.E., SCHENKE, H.W., JAKOBSSON, M., NITSCHE, F.O., BUYS, G., GOLEBY, B., *et al*. 2013. The International Bathymetric Chart of the Southern Ocean (IBCSO) version 1.0 - a new bathymetric compilation covering circum-Antarctic waters. *Geophysical Research Letters*, **40**, 3111–3117.

BATCHELOR, C.L., MONTELLI, A., OTTESEN, D., EVANS, J., DOWDESWELL, E.K., CHRISTIE, F.D.W. & DOWDESWELL, J.A. 2020. New insights into the formation of submarine glacial landforms from high-resolution autonomous underwater vehicle data. *Geomorphology*, **370**, 107396.

BÖTTNER, C., BERNDT, C., REINARDY, B.T.I., GEERSEN, J., KARSTENS, J., BULL, J.M., *et al*. 2019. Pockmarks in the Witch Ground Basin, central North Sea. *Geochemistry, Geophysics, Geosystems*, **20**, 1698–1719.

BRACHFELD, S., DOMACK, E., KISSEL, C., LAJ, C., LEVENTER, A., ISHMAN, S., *et al*. 2003. Holocene history of the Larsen-A Ice Shelf constrained by geomagnetic paleointensity dating. *Geology*, **31**, 749–752.

BROWN, C.S., NEWTON, A.M.W., HUUSE, M. & BUCKLEY, F. 2017. Iceberg scours, pits, and pockmarks in the North Falkland Basin. *Marine Geology*, **386**, 140–152.

BÜNZ, S., POLYANOV, S., VADAKKEPULIYAMBATTA, S., CONSOLARO, C. & MIENERT, J. 2012. Active gas venting through hydrate-bearing sediments on the Vestnesa Ridge, offshore W-Svalbard. *Marine Geology*, 332–334, 189–197.

CATHLES, L.M., SU, Z. & CHEN, D. 2010. The physics of gas chimney and pockmark formation, with implications for assessment of seafloor hazards and gas sequestration. *Marine and Petroleum Geology*, **27**, 82–91.

CHAND, S., THORSNES, T., RISE, L., BRUNSTAD, H. & STODDART, D. 2016. Pockmarks in the SW Barents Sea and their links with iceberg ploughmarks. *In* Dowdeswell, J.A., Canals, M., Jakobsson, M., Todd, B.J., Dowdeswell, E.K. & Hogan, K.A., *eds*., Atlas of submarine glacial landforms: Modern, Quaternary and Ancient. *Geological Society, London, Memoirs*, **46**, 295–296.

CHRISTIE, F.D.W., BENHAM, T.J., BATCHELOR, C.L., RACK, W., MONTELLI, A. & DOWDESWELL, J.A. 2022. Antarctic ice-shelf advance driven by anomalous atmospheric and sea-ice circulation. *Nature Geoscience*, 10.1038/s41561-022-00938-x.

COOK, A.J. & VAUGHAN, D.G. 2010. Overview of areal changes of the ice shelves on the Antarctic Peninsula over the past 50 years. *The Cryosphere*, **4**, 77–98.

DANDO, P.R., AUSTEN, M.C., BURKE JR, R.A., KENDALL, M.A., KENNICUTT II, M.C., JUDD, A.G., *et al*. 1991. Ecology of a North Sea pockmark with an active methane seep. *Marine Ecology Progress Series*, **70**, 49–63.

DEL VALLE, R.A., YERMOLIN, E., CHIARANDINI, J., GRANEL, A.S. & LUSKY, J.C. 2017. Methane at the NW Weddell Sea, Antarctica. *Journal of Geological Research*, **2017**, 5952916.

DEPOORTER, M.A., BAMBER, J.L., GRIGGS, J., LENAERTS, J.T.M., LIGTENBERG, S.R.M., VAN DEN BROEKE, M.R. & MOHOLDT, G. 2013. Synthesized grounding line and ice shelf mask for Antarctica. *PANGAEA*. Retrieved from https://doi.org/10.1594/PANGAEA.819151.

DOMACK, E., ISHMAN, S., LEVENTER, A., SYLVA, S., WILLMOTT, V. & HUBER. B. 2005. A chemotrophic ecosystem found beneath Antarctic Ice Shelf. *EOS Transactions of the American Geophysical Union*, **86**, 269–276.

DOWDESWELL, J.A. & VÁSQUEZ, M. 2013. Submarine landforms in the fjords of southern Chile: implications for glacimarine processes and sedimentation in a mild glacier-influenced environment. *Quaternary Science Reviews*, **64**, 1–19.

DOWDESWELL, J.A., BATCHELOR, C.L., MONTELLI, A., OTTESEN, D., CHRISTIE, F.D.W., DOWDESWELL, E.K. & EVANS, J. 2020a. Delicate seafloor landforms reveal rapid Antarctic grounding-line retreat of kilometres per year. *Science*, **368**, 1020–1024.

DOWDESWELL, J.A., BATCHELOR, C.L., DORSCHEL, B., BENHAM, T.J., CHRISTIE, F.D.W., DOWDESWELL, E.K., *et al*. 2020b. Sea-floor and sea-ice conditions in the western Weddell Sea, Antarctica, around the wreck of Sir Ernest Shackleton's *Endurance*. *Antarctic Science*, **32**, 301–313.

EVANS, J., PUDSEY, C.J., Ó COFAIGH, C., MORRIS, P.W. & DOMACK, E.W. 2005. Late Quaternary glacial history, dynamics and sedimentation of the eastern margin of the Antarctic Peninsula Ice Sheet. *Quaternary Science Reviews*, **24**, 741–774.

GARCÍA, M., ERCILLA, G. & ALONSO, B. 2009. Morphology and sedimentary systems in the Central Bransfield Basin, Antarctic Peninsula: sedimentary dynamics from shelf to basin. *Basin Research*, **21**, 295–314.

GIUSTINIANI, M., TINIVELLA, U., SAULI, C. & DELLA VEDOVA, B. 2017. Distribution of the gas hydrate stability zone in the Ross Sea, Antarctica. *Andean Geology*, **45**, 78–86.

HOFFMANN, J.J.L., SCHNEIDER VON DEIMLING, J., SCHRÖDER, J.F., SCHMIDT, M., HELD, P., CRUTCHLEY, G.J., *et al*. 2020. Complex eyed pockmarks and submarine groundwater discharge revealed by acoustic data and sediment cores in Eckernförde Bay, SW Baltic Sea. *Geochemistry, Geophysics, Geosystems*, **21**, e2019GC008825.

HOVLAND, M. 1981. Characteristics of pockmarks in the Norwegian Trench. *Marine Geology*, **39**, 103–117

HOVLAND, M. & JUDD, A. 1988. *Seabed pockmarks and seepages: impact on geology, biology and the marine environment*. Bath: Graham and Trotman Ltd, 293 pp.

HOVLAND, M., GARDNER, J.V. & JUDD, A.G. 2002. The significance of pockmarks to understanding fluid flow processes and geohazards. *Geofluids*, **2**, 127–136.

HOVLAND, M., HEGGLAND, R., DE VRIES, M.H. & TJELTA, T.I. 2010. Unit-pockmarks and their potential significance for predicting fluid flow. *Marine and Petroleum Geology*, **27**, 1190–1199.

HOWAT, I.M., PORTER, C., SMITH, B.E., NOH, M.-J. & MORIN, P. 2019. The Reference Elevation Model of Antarctica. *The Cryosphere*, **13**, 665–674.

JUDD, A. & HOVLAND, M. 2009. *Seabed fluid flow: the impact on geology, biology and the marine environment*. Cambridge: Cambridge University Press, 475 pp.

LAVOIE, C., DOMACK, E.W., PETTIT, E.C., SCAMBOS, T.A., LARTER, R.D., SCHENKE, H.-W., *et al*. 2015. Configuration of the northern Antarctic Peninsula Ice Sheet at LGM based on a new synthesis of seabed imagery. *The Cryosphere*, **9**, 613–629.

LAWVER, L., LEE, J., KIM, Y. & DAVEY, F. 2012. Flat-topped mounds in western Ross Sea: carbonate mounds or subglacial volcanic features. *Geosphere*, **8**, 645–653.

MAJOROWICZ, J.A. & OSADETZ, K.G. 2001. Gas hydrate distribution and volume in Canada. *American Association of Petroleum Geologists Bulletin*, **85**, 1211–1230.

Mazzini, A., Svensen, H.H., Planke, S., Forsberg, C.F. & Tjelta, T.I. 2016. Pockmarks and methanogenic carbonates above the giant Troll gas field in the Norwegian North Sea. *Marine Geology*, **373**, 26–38.

Nicholls, K.W., Østerhus, S., Makinson, K., Gammelsrød, T. & Fahrbach, E. 2009. Ice-ocean processes over the continental shelf of the southern Weddell Sea, Antarctica: a review. *Reviews of Geophysics*, **47**, 2007RG000250.

Niemann, H., Fischer, D., Graffe, D., Knittel, K., Monteil, A., Heilmayer, O., *et al*. 2009. Biogeochemistry of a low-activity cold seep in the Larsen B area, western Weddell Sea, Antarctica. *Biogeosciences*, **6**, 2383–2395.

Ó Cofaigh, C., Davies, B.J., Livingston, S.J., Smith, J.A., Johnson, J.S., Hocking, E.P., *et al*. 2014. Reconstruction of ice-sheet changes in the Antarctic Peninsula since the Last Glacial Maximum. *Quaternary Science Reviews*, **100**, 87–110.

Smith, R.T. & Anderson, J.B. 2010. Ice-sheet evolution in James Ross Basin, Weddell Sea margin of the Antarctic Peninsula: the seismic stratigraphic record. *GSA Bulletin*, **122**, 830–842.

Solheim, A. & Elverhøi, A. 1993. Gas-related sea floor craters in the Barents Sea. *Geo-Marine Letters*, **13**, 235–243.

Vernet, M., Geibert, W., Hoppema, M., Brown, P.J., Haas, C., Hellmer, H.H., *et al*. 2019. The Weddell Gyre, Southern Ocean: present knowledge and future challenges. *Reviews of Geophysics*, **57**, 623–708.

Wadham, J.L., Arndt, S., Tulaczyk, S., Stibal, M., Tranter, M., Telling, J., *et al*. 2012. Potential methane reservoirs beneath Antarctica. *Nature*, **488**, 633–637.

Wadham, J.L., Hawkings, J.R., Tarasov, L., Gregoire, L.J., Spencer, R.G.M., Gutjahr, M., *et al*. 2019. Ice sheets matter for the global carbon cycle. *Nature Communications*, **10**, 3567.

Webb, K.E., Barnes, D.K.A. & Planke, S. 2009. Pockmarks: Refuges for marine benthic biodiversity. *Limnology and Oceanography*, **54**, 1776–1788.

Winsborrow, M., Andreassen, K., Hubbard, A., Plaza-Faverola, A., Gudlaugsson, E. & Patton, H. 2016. Regulation of ice stream flow through subglacial formation of gas hydrates. *Nature Geoscience*, **9**, 370–374.